Investigation of Flow Instability in Two-Phase Natural Circulation – Experimental and Numerical Results

Chaiwat MUNCHAROEN, Department of Nuclear Technology, Chulalongkorn University, Phyathai Rd., Patumwan, Bangkok, Thailand 10330 Tel: 02-2186781 Email: cmunchar@chula.com

Tatchai SUMITRA, Department of Nuclear Technology, Chulalongkorn University, Phyathai Rd., Patumwan, Bangkok, Thailand 10330

Sunchai NILSUWANKOSIT, Department of Nuclear Technology, Chulalongkorn University, Phyathai Rd., Patumwan, Bangkok, Thailand 10330

ABSTRACT

The experiment has been conducted to investigate the effect of heat flux, pressure and subcooling on the proposed channel configuration in the two-phase natural circulation. The numerical model has been developed by using two-fluid model written in FORTRAN programming language to investigate the effect of flow characteristics on flow instability of two-phase natural circulation caused by boiling. The time step is fixed at 1 millisecond at all time and the mesh size is 100 mm. The semi-implicit scheme is utilized for finite difference equations. Newton Block Gauss Seidel (NBGS) method is employed to solve the system equations for unknown variables. Then the numerical results are analyzed and verified with the experimental results. It is found that the numerical and experimental results are in good agreement. More importantly, for this experimental geometry the new map of the occurrence of the geysering at the pressure higher than 0.35 MPaA is discovered.

1. Introduction

Natural circulation is the phenomenon, which can be found in many industries such as in the riser tubes of the steam generators and in the boiler tubes of the power plants or in the coolant channels between the nuclear fuel elements in a boiling water reactor[1]. The buoyancy effect due to heat transfer from the fuel rods induces the circulation of the water[2]. In nuclear industry, the Simplified Boiling Water Reactor (SBWR)[3] has a promising prospect regarding to competitive power generation cost, shortened construction time and simpler safety systems. The method of natural circulation is proposed as an important feature to remove the heat dissipated from the core. By eliminating the recirculating pumps, the potential accident resulted from the recirculating pumps trip will be eliminated. However, SBWR will face some instabilities and oscillations during the start-up operation due to the occurrence of void fractions in the system. This will have an effect on reactor reactivity. Moreover, SBWR geometry might influence the stability of the system in case of insufficient vaporization.

The study of flow instabilities is important because of their effects on heat transfer characteristic, flow characteristics, which may lead to physical damage in the boiling water reactor core[4]. The major kinds of instabilities in nuclear industry including flow excursion, geysering, natural circulation and density wave have been extensively investigated analytically and experimentally in the past. The classification of the two-phase flow instabilities was reviewed by Boure et al.[5]. Aritomi et al.[6-7] investigated flow instabilities analytically and experimentally in a parallel channel in boiling vertical upflow system. A non-linear analytical model was developed to explain the instabilities in a parallel channel. The results from this model were in good agreement with the experimental results. Due

RECEIVED 31 October, 2002

ACCEPTED 16 May, 2003

to the advance in computer technology, many researchers have developed new numerical codes using the homogeneous, drift-flux or two-fluid models to investigate the instabilities in boiling channels. The well-known codes in nuclear fields such as TRAC, RELAP5, RETRAN, CATHARE and CATHENA mostly utilize the finite difference or finite volume scheme with implicit, explicit or semi-implicit method to replace the derivatives in differential equations and turn into algebraic equations. In this scheme the void fraction, pressure, energy or scalar value will be calculated at the cell center and the velocity will be calculated at the cell boundaries. The two-fluid model employs six conservation equations of mass, momentum and energy for each phase. It requires the interaction between the liquid and vapor phase such as interfacial mass transfer and interfacial friction. In nuclear industry, due to the importance of the two-phase flow instability on the operation of the nuclear reactor it is still need the good model to predict the instabilities, which may occur in the system.

The objective of this paper is to illustrate the method to develop two-fluid model, investigate and analyze the results from numerical model and experimental facility. The model of two-phase flow to simulate the natural circulation in a boiling channel in SBWR is developed by using the two-fluid model. In this model, the time step is kept constant at 1 millisecond at all time and the mesh size is fixed at 100 mm. Then the experiment is conducted to get the results to verify the results from the numerical model.

2. Mathematical Analysis

The two-fluid model is developed using the equations employed in RELAP5/MOD3.2[8]. It employs the six equations of mass, momentum and energy for each phase as follows:

Vapor and Liquid Mass Equations:

$$\frac{\partial}{\partial t}(\alpha_l \rho_l) + \frac{1}{A}\frac{\partial}{\partial z}(\alpha_l \rho_l V_l A) = \Gamma_l \quad (1)$$

$$\frac{\partial}{\partial t}(\alpha_g \rho_g) + \frac{1}{A}\frac{\partial}{\partial z}(\alpha_g \rho_g V_g A) = \Gamma_g \quad (2)$$

Vapor and Liquid Momentum Equations:

$$\alpha_l \rho_l A\frac{\partial V_l}{\partial t} + \frac{1}{2}\alpha_l \rho_l A\frac{\partial V_l^2}{\partial z} = -\alpha_l A\frac{\partial P}{\partial z} + \alpha_l \rho_l AB_z - (\alpha_l \rho_l A)FWF(V_l) - \Gamma_g A(V_{lI} - V_l) - (\alpha_l \rho_l A) FIF(V_l - V_g) - C\alpha_l \alpha_g \rho_m A\left[\frac{\partial (V_l - V_g)}{\partial t} + V_g\frac{\partial V_l}{\partial z} - V_l\frac{\partial V_g}{\partial z}\right] \quad (3)$$

$$\alpha_g \rho_g A\frac{\partial V_g}{\partial t} + \frac{1}{2}\alpha_g \rho_g A\frac{\partial V_g^2}{\partial z} = -\alpha_g A\frac{\partial P}{\partial z} + \alpha_g \rho_g AB_z - (\alpha_g \rho_g A)FWG(V_g) + \Gamma_g A(V_{gI} - V_g) - (\alpha_g \rho_g A) FIG(V_g - V_l) - C\alpha_g \alpha_l \rho_m A\left[\frac{\partial (V_g - V_l)}{\partial t} + V_l\frac{\partial V_g}{\partial z} - V_g\frac{\partial V_l}{\partial z}\right] \quad (4)$$

Vapor and Liquid Energy Equations:

$$\frac{\partial}{\partial t}(\alpha_l \rho_l U_l) + \frac{1}{A}\frac{\partial}{\partial z}(\alpha_l \rho_l U_l V_l A) = -P\frac{\partial \alpha_l}{\partial t} - \frac{P}{A}\frac{\partial}{\partial z}(\alpha_l V_l A) + Q_{wl} + Q_{il} - \Gamma_{ig}h_l^* - \Gamma_w h_l' + DISS_l \quad (5)$$

$$\frac{\partial}{\partial t}(\alpha_g \rho_g U_g) + \frac{1}{A}\frac{\partial}{\partial z}(\alpha_g \rho_g U_g V_g A) = -P\frac{\partial \alpha_g}{\partial t} - \frac{P}{A}\frac{\partial}{\partial z}(\alpha_g V_g A) + Q_{wg} + Q_{ig} + \Gamma_{ig}h_g^* + \Gamma_w h_g' + DISS_g \quad (6)$$

In two-fluid model, due to the existence of the liquid and vapor phase the interfacial mass transfer and interfacial friction have to be included. Moreover, the interfacial heat transfer and heat transfer coefficients are required to simulate the heat transfer from the fuel rods in the reactor core. The constitutive and state equations used in this model can be found in reference [9].

3. Semi-implicit Scheme

The semi-implicit scheme is employed by replacing the system of difference equations with a system of finite-difference partially implicit in time. In this scheme, some important parameters are taken by the ones in the new time step by adding increment to present initial values. To derive the finite difference equations, the concept of control volume (or mesh cell) is used. The control

volumes are separated into mass and energy control volumes and momentum control volume. The velocities of momentum control volume will be calculated at the boundaries of mass and energy control volume. This will result in forming a staggered spatial mesh, which the scalar properties i.e. pressure, energy and void fraction are defined at cell centers and the vector properties i.e. velocities are defined at the cell boundaries.

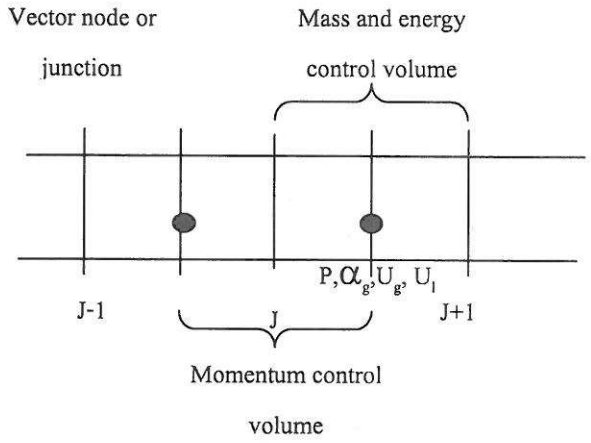

Figure 1 Semi-implicit Scheme

To derive the finite difference equations, the semi-implicit scheme shown in Figure 1 is employed in the two-fluid model. To calculate the liquid and vapor velocity of the two-fluid model, the sum of Equation (3) and (4), the difference of Equation (3) and (4) are expressed as:

Sum of liquid and vapor momentum equations:

$$\alpha_g\rho_g A\frac{\partial v_g}{\partial t}+\alpha_l\rho_l A\frac{\partial v_l}{\partial t}+\frac{1}{2}\alpha_g\rho_g A\frac{\partial v_g^2}{\partial z}+\frac{1}{2}\alpha_l\rho_l A\frac{\partial v_l^2}{\partial z}$$
$$=-A\frac{\partial P}{\partial z}+\rho_m B_z A-(\alpha_g\rho_g A)FWG(v_g)-(\alpha_l\rho_l A)FWF(v_l) \quad (7)$$
$$-\Gamma_g A(v_g-v_l)$$

Difference of liquid and vapor momentum equations:

$$(1+C\rho_m^2/\rho_g\rho_l)A\left[\frac{\partial v_g}{\partial t}-\frac{\partial v_l}{\partial t}\right]+\frac{1}{2}A\frac{\partial v_g^2}{\partial z}+\frac{1}{2}A\frac{\partial v_l^2}{\partial z}$$
$$=-A\left(\frac{1}{\rho_g}-\frac{1}{\rho_l}\right)\frac{\partial P}{\partial z}-(FWG(v_g)A-FWF(v_l)A)-\rho_m FI(v_g-v_l)A \quad (8)$$
$$+\Gamma_g A[\rho_m v_l-(\alpha_l\rho_l v_g-\alpha_g\rho_g v_l)]/(\alpha_g\rho_g\alpha_l\rho_l)$$

4. Solution Procedure

The solution procedure used in the drift-flux model and the two-fluid model involves a semi-implicit difference of the field equations and a variation of the Newton Block Gauss Seidel (NBGS) method for solving at each time level the resulting system of algebraic equations[10]. In this method, all equations including difference and constitutive equations, which can be found in Reference 9, are linearized around the latest iterative values of the unknowns. Then all unknowns except void fraction, pressure, liquid internal energy, vapor internal energy, liquid velocity and vapor velocity are eliminated. Because the sum and the difference momentum of liquid and vapor equations couple only single velocity and two pressures, the velocity can be eliminated from these equations in favor of pressures. For the two-fluid model the liquid and vapor mass, the liquid internal energy and the vapor internal energy equations coupling with the sum and the difference momentum equations are arranged orderly. The unknown variables will be void fraction, pressure and liquid internal energy, respectively. The coefficient of the matrix in Figure 2 is factored as

$$M=L+D+U \quad (9)$$

where L and U are lower and upper triangular matrices and D contains the diagonal blocks of M. By using NBGS iteration, the equivalent equation can be expressed as

$$(L+D)X^{k+1}=UX^k+b \quad (10)$$

where X is the unknown variables in Figure 2 and k is the superscripts to indicate the successive iteration approximations. The unknown variables can be achieved easily by inverted the 4x4 blocks diagonal matrix.

$$\begin{bmatrix} D & D & D & 0U & 0 & & & \\ D & D & D & 0U & 0 & & & \\ D & D & D & 0U & 0 & & & \\ D & D & D & 0U & 0 & & & \\ 0L & 0 & D & D & D & 0U & 0 & \\ 0L & 0 & D & D & D & 0U & 0 & \\ 0L & 0 & D & D & D & 0U & 0 & \\ 0L & 0 & D & D & D & 0U & 0 & \\ . & & & & & & & \\ . & & & & & & & \end{bmatrix} \begin{bmatrix} \alpha_1 \\ P_1 \\ el_1 \\ ev_1 \\ \alpha_2 \\ P_2 \\ el_2 \\ ev_2 \\ . \\ .. \end{bmatrix} = [b]$$

Figure 2 Structure of the set of algebraic equations

5. Numerical and Experimental results and discussions

The configuration of the test section is shown in Figure 3. The experimental apparatus consists of lower plenum, channel test sections, upper plenum, upper tank, down-comer pipe and by-pass line. The water is used as the test fluid. The diameter of the inner rod, which is assumed to be the fuel, is 10 mm provided with the heater. The outer wall diameter is 20.0 mm. The channel length is 2500 mm. and the heated channel is 1200 mm. The non-heated region is 300 and 1000 mm. at the inlet and outlet of the channels, respectively. To investigate the flow characteristic at first the exit pressure is fixed at 0.1 MPaA and the inlet subcooling is fixed at 5 K. The heat flux provided by the heater is increased from 0-600 kW/m^2. Then the exit pressure is changed from 0.1, 0.2, 0.4, 0.5, 0.7 MPaA. After that the inlet subcooling is changed from 5 to 10 to 15 K.

5.1 Effect of System pressure

The system pressure is varied from 0.1, 0.2, 0.4, 0.5 and 0.7 MPaA to investigate the effect of the system pressure at subcooling 10 K. Figure 4-7 show the effect of pressure on average total inlet velocity, average channel velocity, amplitude of velocity and amplitude of pressure drop, respectively. The average total inlet velocity and the average channels velocity increased sharply at the heat flux from 100 to 400 kW/m^2 and gradually increased after that. Aritomi[6] showed that the average total inlet velocity and the average channels velocity decreased as the pressure system increased. However, from these experiments the average total inlet velocity and the average channels velocity had the tendency to decrease with the increase in system pressure, shown in Figure 5, from 0.1 MPaA to 0.7 MPaA except at the pressure 0.4 and 0.2 MPaA, respectively. Figure 6-7 show that the amplitude of the velocity and the amplitude of the pressure drop have the trend to decrease as the system pressure increase except at the pressure 0.4 MPaA.

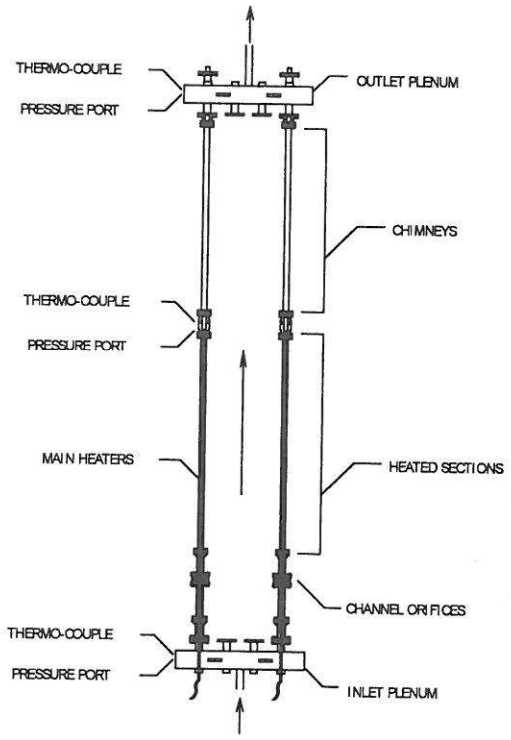

Figure 3 Test section

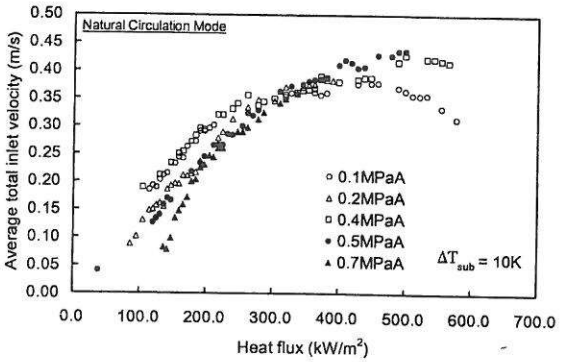

Figure 4 Effect of pressure on average total inlet velocity and heat flux

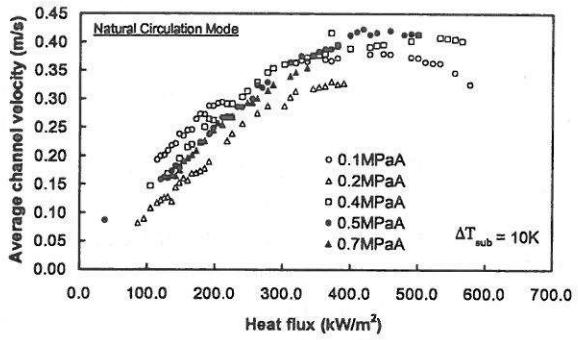

Figure 5 Effect of pressure on average channel velocity and heat flux

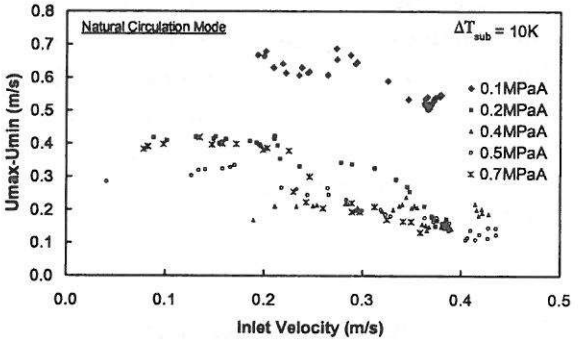

Figure 6 Effect of pressure on the amplitude of the velocity and inlet velocity

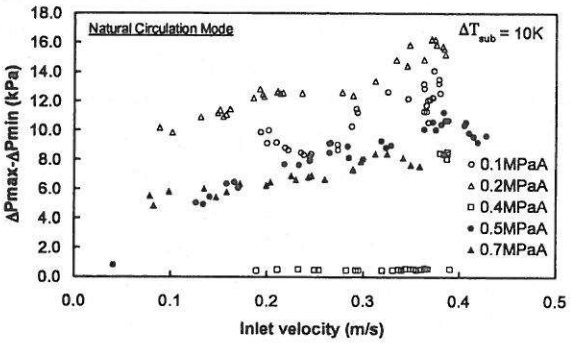

Figure 7 Effect of pressure on amplitude of pressure drop and inlet velocity

Chiang[11] found that the geysering was not observed at the pressure above 0.35 MPaA. However, in these experiments it is interesting that the geysering, which had the characteristic of bubble rising and condensing at the outlet plenum following by the flow reversal in the test section, was observed up to 0.7 MPaA as shown on the flow instability map in Figure 8. The reason for this phenomenon is due to the riser effect on the condensation of the coolant in the test channels. The longer riser induces a large magnitude of the amplitude of the velocity because the geysering is more pronounced in longer risers. Thus the 1 meter long riser in this experiment gives rise to the occurrence of the geysering above 0.35 MPaA. The detail of the phenomenon due to the effect of channel geometry will be described in the next section.

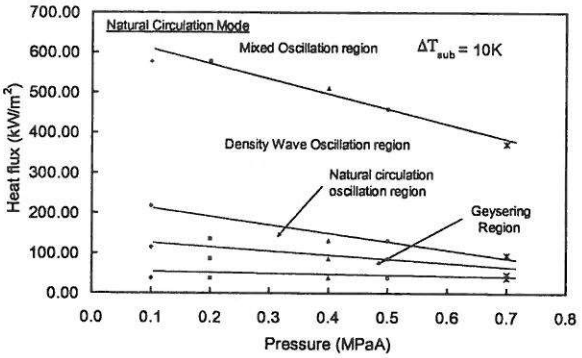

Figure 8 Flow instability map

5.2 Effect of Subcooling

The effect of subcooling at 5, 10 and 5 K is investigated at pressure 0.1 MPaA. It is found that the average total inlet velocity, the average channel velocity decrease at increasing subcooling as shown in Figure9-10. In general the increasing subcooling will lower the Grashof number and liquid temperature and thus reduce the heat transfer coefficient and interfacial heat transfer coefficient, respectively. As the heat and the mass transfer between liquid and vapor phases decrease, the average total inlet velocity and the average channel velocity decrease. The increase in subcooling has an effect on increase non-boiling length and decrease void fraction. In Figure11-12 the amplitude of the velocity, the amplitude of pressure drop decrease with an increasing subcooling at low heat flux, respectively. The amplitude of the average channel velocity has the tendency to decrease with the increasing subcooling at low heat flux.

In Contrast the amplitude of the average channel velocity the amplitude of the pressure drop increases with the increasing inlet velocity and has the tendency to decrease with the increasing subcooling at low heat flux.

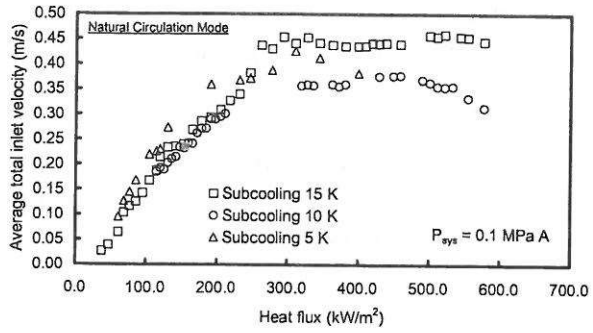

Figure 9 Effect of subcooling on average inlet velocity

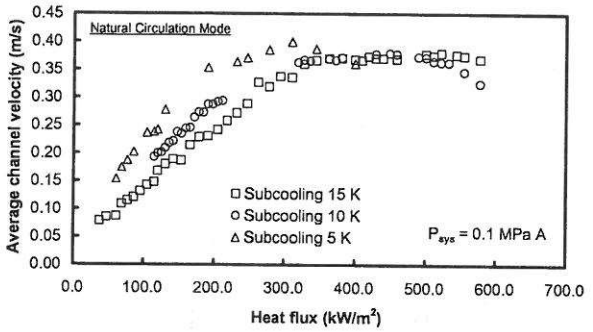

Figure 10 Effect of subcooling on average channel velocity

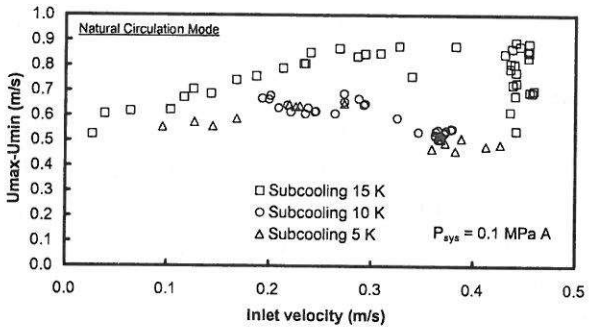

Figure 11 Effect of subcooling on amplitude of velocity

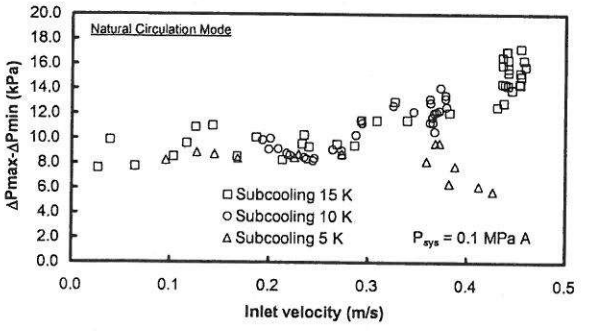

Figure 12 Effect of subcooling on amplitude of pressure drop

5.3 Effect of Channel Geometry

As mentioned in the previous section that the length of the riser has the effect on the occurrence of the geysering at the pressure above 0.35 MPaA, Figure 3 shows the test section with the heater inside connected to the 1 meter long riser and the upper plenum. The slug bubble has the high velocity in the test section due to the annular shape between the test section and the heater. Because of the circular shape of the riser when the slug bubble enters into the riser, the shape of the slug bubble changes and the velocity of the slug bubble decreases. At the point where the pressure head increases, it is easier for the slug bubble to collapse before entering at the upper plenum. This makes the geysering occurring at the higher pressure.

6. Comparison of Numerical and Experimental Results

The two-fluid model is developed to simulate the same configuration of the experiment apparatus. The time step is kept constant at 1 millisecond at all time. The spatial mesh size is fixed at 100 mm. The uniform mesh size is employed at the test section. The numerical model is performed at the pressure 0.1 MPaA and subcooling 10 K. The two-fluid model will be modified to this benchmark. Then it will be utilized to perform the steady state and transient conditions. The results from the two-fluid model and experiment, shown in Figure13-16, display that they are in good agreement.

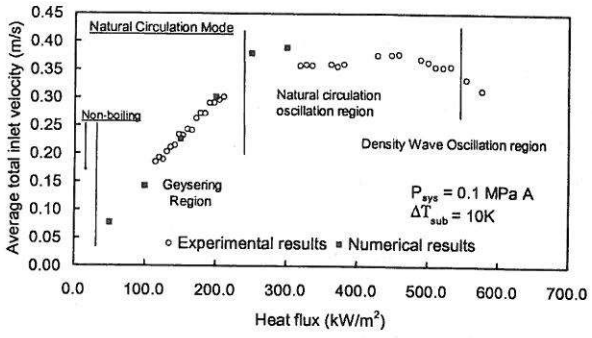

Figure 13 Numerical and experimental results of average total inlet velocity and heat flux

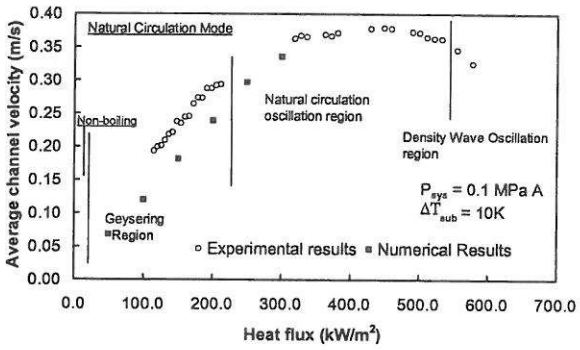

Figure 14 Numerical and experimental results of average channel velocity and heat flux

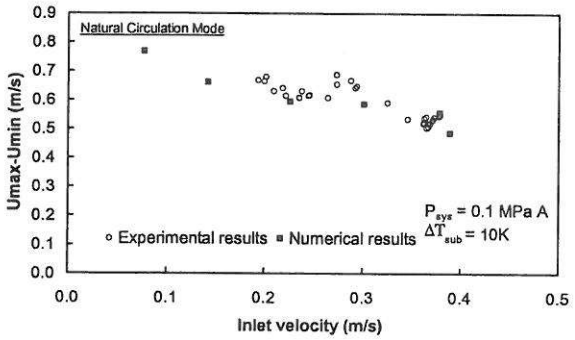

Figure 15 Numerical and experimental results of amplitude of the velocity and inlet velocity

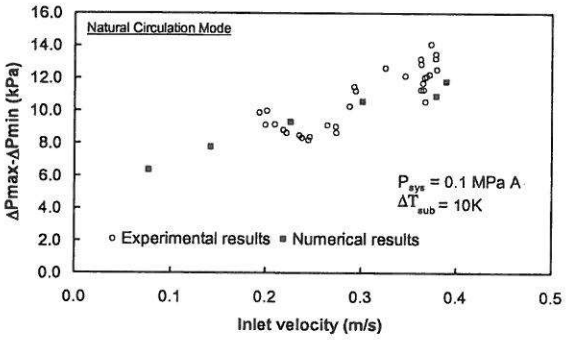

Figure 16 Numerical and experimental results of amplitude of pressure drop and inlet velocity

7. Conclusions

The two-fluid model has been developed to investigate the two-phase flow instability in a natural boiling channel. The semi-implicit finite difference scheme is employed to turn into the algebraic equations and the Newton Block Gauss Seidel (NBGS) is utilized to provide the solution of the numerical models. It is found that the numerical and experimental results are in good agreement. More importantly, the geysering can occur at the pressure higher than 0.35 MPaA with this experimental geometry.

Acknowledgments

The author would like to acknowledge the financial support from the Thailand Research Fund through the Royal Golden Jubilee Ph.D. program (Grant No. PHD/00122/2541) and appreciate to Prof. Dr. M.Aritomi for his partially financial support, kind advice and supervision in Tokyo Institute of Technology.

Nomenclature

A : Cross sectional area (m^2)

B_z : Body force in z coordinate direction (m/s^2)

C : Coefficient of virtual mass

FI : Interphase drag coefficient (m^3/kg-s)

FIF , FIG : Interphase drag coefficients of liquid and vapor (s^{-1})

FWF , FWG : Wall drag coefficients of liquid and vapor (s^{-1})

f : Oscillation frequency (Hz)

$DISS$: Energy dissipation function (W/m^3)

P : Pressure (Pa)

Q : Volumetric heat addition rate (W/m^3)

Δt : Mesh time (s)

u_g : Velocity of gas phase (m/s)

u_l : Velocity of liquid phase (m/s)

u_{in} : Inlet velocity (m/s)

vol : Volume of one cell (m^3)

Δz : Volume mesh (m)

Greek

ρ_g : Specific density of gas phase (kg/m^3)

ρ_l : Specific density of liquid phase (kg/m^3)

α : Void fraction (-)

Γ : Mass transfer rate (kg/m^3-s)

τ : Shear stress (N)

Superscript

$*$: Bulk property

s :Saturation property

Subscript

g : Gas phase

(i) : i cell

I : Interface

in : Inlet

ig : Interphase to gas

l : Liquid phase

m : Mixture

max: Maximum

min: Minimum

w :Wall

References

[1] M.L. Corradini, "General introduction and concepts", Multiphase flow and heat transfer for industrial application, May 17-19,(1988)

[2] G. Kocamustafaogullari, "Flow patterns predictions", Multiphase flow and heat transfer for industrial application, May 17-19, (1988)

[3] J.D. Duncan, "SBWR, A simplified boiling water reactor", Nucl. Eng. Des. 109, pp.73-77, (1988)

[4] V. Chatoorgoon, "SPORTS- A Simple non-linear thermalhydraulic stability code", Nucl. Eng. Des. 93, pp.51-67, (1986)

[5] J.A. Boure, A.E. Bergles and L.S. Tong, "Review of two-phase flow instability", Nucl. Eng. Des. 25, pp.165-192, (1973)

[6] M. Aritomi, S. Aoki and A. Inoue, "Thermo-hydraulic instabilities in parallel boiling channel systems Part 1. A non-linear and a linear analytical model", Nuc. Eng. Des..95, pp. 105-116, (1986)

[7] M. Aritomi, S. Aoki and A. Inoue, "Thermo-hydraulic instabilities in parallel boiling channel systems Part 2. Experimental results", Nuc. Eng. Des..95, pp.117-127, (1986)

[8] V.H. Ransom et al., "RELAP5/MOD3.2 code manual, volume 1:code structure, system models, and solution methods", NUREG/CR5535-V1, (1995)

[9] C. Muncharoen, S. Nilsuwankosit and T. Sumitra, "The effect of flow loop conditions on stabilities of two-phase natural circulation caused by boiling-(I) Modeling development", Proceeding of the 8th Conference on Nuclear Science and Technology, June 21-22, Bangkok, Thailand , (2001)

[10]D.R.Liles and Wm.H.Reed, "A Semi-implicit Method for Two-Phase Fluid Dynamics", J. Comp. Phys. 26, pp.390-407, (1978)

[11]J.H. Chiang, "Thermo-hydraulics during start-up in natural circulation boiling water reactor", Ph.D. dissertation, (1994)